

# Invisible Higgs in theories of large extra dimensions

Anindya Datta<sup>a</sup>, Katri Huitu<sup>b,c</sup>, Jari Laamanen<sup>b</sup>, and Biswarup Mukhopadhyaya<sup>d</sup>

<sup>a</sup>INFN, Sezione di Roma, Universita La Sapienza  
P. le A. Moro 2, Rome I-00185, Italy

<sup>b</sup>Helsinki Institute of Physics  
P.O.Box 64, FIN-00014 University of Helsinki, Finland

<sup>c</sup>High Energy Physics Division, Department of Physical Sciences,  
P.O.Box 64, FIN-00014 University of Helsinki, Finland

<sup>d</sup>Harish Chandra Research Institute, Chhatnag Road, Jhusi  
Allahabad - 211 019, India

## Abstract

We discuss the possibility of detecting a Higgs boson in future collider experiments if large extra dimensions are realized in nature. In such a case, the Higgs boson can decay invisibly by oscillating into a graviscalar Kaluza-Klein (KK) tower. We show that the search for such a Higgs at an  $e^+e^-$  linear collider entails more complications than are usually thought of in relation to an invisibly decaying Higgs, the main sources of such complications being the simultaneous presence of a continuum graviton production and the broadening of the Higgs peak. We discuss possible ways of overcoming such difficulties, and conclude that the detection of such a Higgs boson might still be a problem beyond the mass range of 250-300 GeV.

## 1 Introduction

Confirming the Higgs mechanism as the underlying principle of electroweak symmetry breaking is one of the main goals of upcoming accelerators. It is expected that the Large Hadron Collider (LHC) will detect the particle responsible for the symmetry breaking in the Glashow-Salam-Weinberg model, namely, the Higgs  $H$ . However, for studying its properties in detail, a linear electron-positron collider will probably be needed.

The strategy for Higgs search depends on the decay branching fractions of Higgs to different channels. This is where the likely modification of Higgs signals due to physics beyond the Standard Model (SM) comes up for consideration, since such new physics is very likely to affect the Higgs interactions rates and its consequent decay products in various ways. One somewhat

bizarre (but by no means inconceivable) possibility in this context is that a Higgs can have a substantial branching ratio for decay into invisible final states. This possibility has been underlined in a number of well-motivated theoretical options [1, 2, 3, 4, 5, 6, 7, 8].

It is expected in some of these options that such invisible decays will dominate, making the Higgs boson difficult to identify in collider experiments. It is therefore a rather interesting subject of investigations as to the nature and extent of invisibility acquired by Higgs, and how it can be related to specific aspects of the theories concerned, whether it be supersymmetry [4], majoron models [5, 6] or models with extra compact spacelike dimensions [7, 8]. Our interest in this paper is to study the invisible decay modes suggested in models with extra dimensions.

Theories of the aforementioned type have been popular in recent times, because (a) they offer a rather appealing solution to the hierarchy problem, and (b) they entail the prospect of testing gravitational effects in TeV-scale experiments.. Broadly two such types of models have been studied so far, namely, the Arkani-Hamed-Dimopoulos-Dvali (ADD) [9] and Randall-Sundrum (RS) [10] types. Both of them envisage extra compact spacelike dimensions, with gravity propagating in the ‘bulk’, while all the SM fields are confined to (3+1) dimensional slices or ‘branes’ in the minimal versions of both types. In ADD-type models, one has a factorizable geometry, where the projection on the brane leads to a continuum of scalar and tensor graviton states, whose cumulative effect gives new contributions at the TeV scale, thus providing a natural cut-off to SM physics. In RS-type models, on the other hand, a non-factorizable geometry is assumed, where the size of the fifth dimension is small and hierarchy is removed by a ‘warp’ factor with a large negative exponent, which scales down large mass parameters on the visible brane. The discussion in this note is related to the former type of models.

An important feature of these models is that the Higgs boson can mix with the graviscalars (the tower of scalar states arising out of the projection of the graviton on the visible brane). Although it is not usually retained in the minimal model, it is perfectly consistent with general covariance to augment the four-dimensional effective action with a term

$$S = -\xi \int d^4x \sqrt{-g_{ind}} R(g_{ind}) H^\dagger H, \quad (1)$$

where  $H$  is the Higgs doublet,  $\xi$  is a dimensionless mixing parameter,  $g_{ind}$ , the induced metric on the brane and  $R$  is the Ricci scalar. As has been shown in [7], this term basically arises from the fact that the energy-momentum tensor  $T_{\mu\nu}$  can be extended by a term of the type  $\xi(\eta_{\mu\nu}\partial_\alpha\partial^\alpha - \partial_\mu\partial_\nu)$  while it is still conserved. Once electroweak symmetry is broken, the coupling of the trace of the additional part to the graviscalars leads to a mixing between the physical Higgs field ( $h$ ) and each member of the graviscalar tower. One can parametrize such mixing by the following term in the Lagrangian:

$$\mathcal{L}_{mix} = \frac{1}{M_P} m_{mix}^3 h \sum_n S_n, \quad (2)$$

where,  $m_{mix}^3 = 2\kappa\xi v m_h^2$ ,  $M_P$  is the reduced Planck mass, and  $v$  is the Higgs vacuum expectation value.  $\kappa$  can be expressed in terms of the number of extra dimensions:

$$\kappa \equiv \sqrt{\frac{3(\delta - 1)}{\delta + 2}} \quad (3)$$

$\delta$  being the number of extra compact spacelike dimensions.

It should be mentioned here that the effects of extra dimensions on the Higgs decay modes are different in the case of large or small extra dimensions. This is due to the different spacing of the KK-towers. In the case of the small extra dimensions the spacing is large, and the observable effect is expected to come from the nontrivial mixing of the Higgs boson with the single graviscalar in the model, called radion [10]. The consequences of radion-Higgs mixing have already been explored in the literature [7, 11]. In the case of the large extra dimensions the major effects are due to the closely spaced KK-levels. These lead to the possibly effective ‘invisible decays’ of the Higgs boson, via oscillation into one or the other state belonging to the quasi-continuous tower of graviscalars [7]. The consequence of this strange phenomenon in the context of collider experiments is our concern in this note.

In recent years the invisible decays of the Higgs boson have been under scrutiny, and methods have been developed to detect the invisible Higgs. These are based on tagging of some other particle than the decay products of the Higgs. Mass limits for a Higgs boson decaying dominantly to invisible particles have also been obtained by the LEP experiments [12]. It is assumed that the Higgs boson is produced in association with a  $Z$ -boson, which decays either to charged leptons or hadrons, and a constraint that the decay products are consistent with the  $Z$  mass is applied. Then the mass limit of  $m_H > 114.4$  GeV can be established. What we wish to emphasize here is that *a scenario, where invisibility is induced by scalar-graviscalar mixing, brings in some additional complications in detecting Higgs signals. Some ways out of such complications are suggested here.*

In section 2 we present the branching ratios for invisible decay in terms of the fundamental parameters of theory. Different aspects of the ensuing Higgs signals in a high-energy  $e^+e^-$  collider are discussed in section 3. We summarise and conclude in section 4.

## 2 Higgs invisible decays with scalar-graviscalar mixing

The usual way to handle a case of mixing (as defined in Eq. (2)) is to diagonalise the mass matrix and define the physical scalar eigenstates. However, due to the presence of an infinite number of members of the graviscalar tower, it is technically difficult to tackle this problem in this way.

Instead, one proceeds by considering the Higgs propagator in the flavour basis itself and incorporating all the insertions induced by the mixing term. This requires one to integrate over a tower of quasi-continuous states. As has been shown in [7], the provision of thus having a large number of real intermediate states inserted leads to the development of an imaginary term in the propagator. This imaginary part can be interpreted as an effective decay width entering into the propagator after the fashion of the Breit-Wigner scheme [7]:<sup>1</sup>

$$\Gamma_G = 2\pi\kappa^2\xi^2v^2\frac{m_h^{1+\delta}}{M_D^{2+\delta}}S_{\delta-1}, \quad (4)$$

where  $M_D$  is the  $(4 + \delta)$ -dimensional Planck scale (also called the string scale) and  $S_{\delta-1}$  is the surface of a unit-radius sphere in  $\delta$  dimensions, given by

$$S_{\delta-1} = \frac{2\pi^{\delta/2}}{\Gamma(\delta/2)} \quad (5)$$

---

<sup>1</sup>Our calculation of the width agrees with [15] where the width is twice the value in [7].

Decay width (GeV) of the Higgs boson						
	$m_D = 1.5$ TeV			$m_D = 3$ TeV		
	$\delta = 2$	$\delta = 3$	$\delta = 4$	$\delta = 2$	$\delta = 3$	$\delta = 4$
$m_h = 120$ GeV	0.62	0.163	0.032	0.044	0.016	0.011
$m_h = 200$ GeV	6.445	4.814	3.918	3.778	3.638	3.608

Table 1: Total decay width of Higgs boson in presence of Higgs-graviscalar mixing with mixing parameter  $\xi = 1$ .

This invisibility can be understood qualitatively in the following way. Due to the presence of the mixing terms, a Higgs boson, once produced, has a finite probability (proportional to  $\xi^2$ ) of oscillating into a quasi-continuous multitude of invisible states, corresponding to the graviscalar tower. Though the mixing between the Higgs and any one of the graviscalar is the same, this transition would be favoured when masses of the Higgs and the corresponding graviscalar are close to each other. The mixing is suppressed by  $M_P$ . But summing the oscillation probabilities over the tower can make the *resulting probability for the Higgs going into one of many graviscalars quite big*. Couplings of each graviscalar to ordinary matter being suppressed by Planck mass, any of the states the Higgs can oscillate into is practically invisible. Thus, the Higgs, once transformed into a graviscalar, becomes invisible and this is reflected in the ‘invisible’ decay width developed by the propagator.

Assuming that the graviton KK tower is the only source of the invisible width in the model, we have plotted in Fig. 1 the invisible branching ratio as a function of the mixing parameter. Two masses for the Higgs boson, namely,  $m_h = 120$  GeV, and  $m_h = 200$  GeV, have been used. The plots have been made for  $M_D = 1.5, 3,$  and  $10$  TeV and for  $\delta=2$ . In Table 1, total Higgs boson widths are presented for two values of  $m_D$ , namely 1.5 and 3 TeV; in presence of Higgs-graviscalar mixing. For  $m_h = 120$  GeV, width of the SM Higgs boson is of the order of  $10^{-3}$  GeV. With the on-set of mixing term, the width has become 0.62 GeV for a more favorable case ( $m_D = 1.5$  TeV,  $\delta = 2$ ), which is evident from the table. The decrement of the width with increasing  $\delta$  can be explained by the steady decrease of number density of graviton states in which the Higgs could oscillate. A closer look to the numbers in the second row (for a Higgs mass of 200 GeV), reveals the importance of  $WW, ZZ$  decay channels for Higgs and the comparative strength of these with invisible channel. Decay width of a 200 GeV SM Higgs boson is nearly 2 GeV. At this mass we see that invisible width is comparable with visible channels.

The message emerging from the above discussion is that this effective invisible decay width grows as  $m_h^3$  for  $\delta = 2$ . This implies that even for ( $m_h < 2m_W$ ) total Higgs decay width can be considerably larger than the Standard Model width which in this range is dominated by the decay to fermion pairs and is proportional to  $m_H$ . As a consequence, even for a light Higgs boson, Higgs resonance may not be very sharp. This fact has to be taken into account when one attempts to reconstruct such a Higgs through the recoil invariant mass peak at a linear electron-positron collider.

Invisible decay of Higgs boson is also possible in models with right-handed neutrinos propagating in the bulk [8]. However, in this article we will confine ourselves to the case of Higgs-graviscalar mixing only.

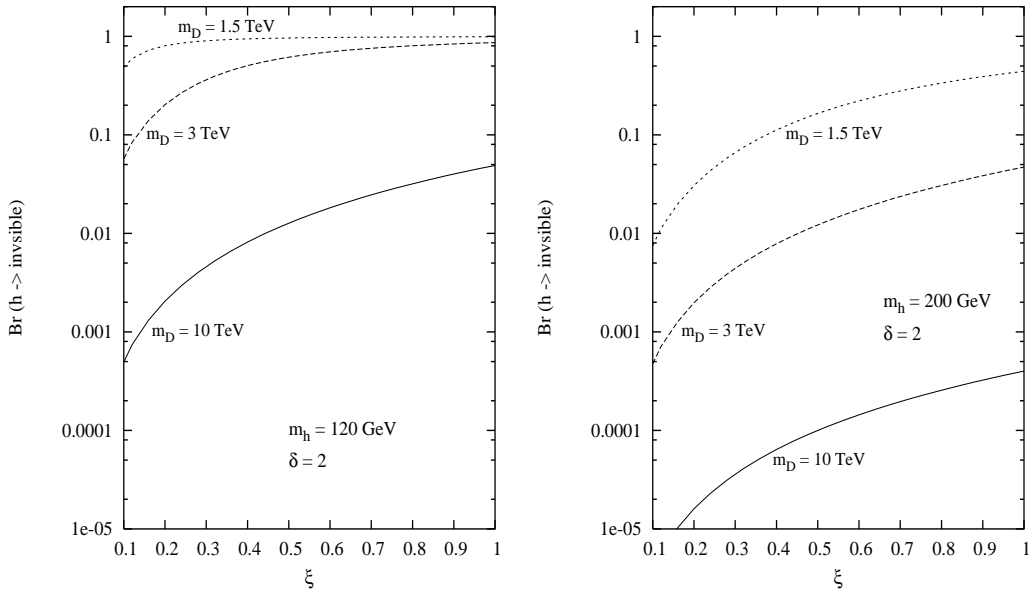


Figure 1: The invisible decay branching ratio of the Higgs boson as a function of the mixing parameter for two representative values of Higgs mass and for number of extra dimension,  $\delta = 2$ .

### 3 $e^+e^-$ colliders

It is evident from the figures presented in the previous section that the Higgs can have a very large invisible branching ratio in the scenario considered here. The identification of such a Higgs at hadron colliders is in general a difficult task; associated productions such as  $WH$  has been studied at Tevatron and LHC [6] only in the context of four dimensional models. The gauge boson fusion (GBF) channel may be interesting at the LHC, but is again plagued with complications, since ADD gravitons can also be produced by the same mechanism. Thus, unless a full and reliable calculation of graviton production is available, the clue on whether an invisible Higgs is produced alongside may be lost from our sight.

We consider the situation at an  $e^+e^-$  machine, where the identification of the recoil mass peak against the  $Z$ -boson in the Bjorken process is widely known to be a reliable method of detecting the Higgs boson. We therefore concentrate on this process, also known as the Higgs-strahlung process, at a linear collider with center of mass energy of 1 TeV,

$$e^+e^- \rightarrow Z(\rightarrow \mu^+\mu^-)h(\rightarrow \text{inv}). \quad (6)$$

The final state we are interested in comprises of a  $\mu^+\mu^-$  pair with missing energy/momentum (corresponding to one or the other of the graviscalars). Due to a sizable Higgs width even for light Higgs bosons, we do not use the narrow width approximation, but rather treat the Higgs boson as a propagator (inclusive of an invisible width) while calculating the cross-section. We have also taken into account the direct graviscalar production alongside.

At the center-of-mass energies we are concentrating on, the production of Higgs boson in  $ZZ$ - and  $WW$ -fusions is also important. However, since we are interested in the invisible decay of the Higgs boson, the  $WW$ -fusion channel is not suitable for our purpose, as in the final state

we are left with an invisibly decaying Higgs with two neutrinos. A closer look at the Higgs production cross-sections [13] in different channels at the  $e^+e^-$  collision reveals that the rate for  $He^+e^-$  in the Higgs-strahlung and  $ZZ$  fusion channels may be comparable for low Higgs masses and center of mass energies higher than 500 GeV. Thus the Higgs/graviscalar production in  $ZZ$ -fusion channel would also contain in the final state a charged lepton pair with an invisibly decaying Higgs. The gravitensor production rate should be fully estimated in the same channel. In the present work, we will report only on the Higgs-strahlung process, which already shows the relative importance of gravitensor and Higgs production, as well as the correlation of 'signal' and 'background' in particular examples of invisible Higgs in extra dimensional models. That is why we have chosen to illustrate our main point by focusing on the  $\mu^+\mu^-$  final state.

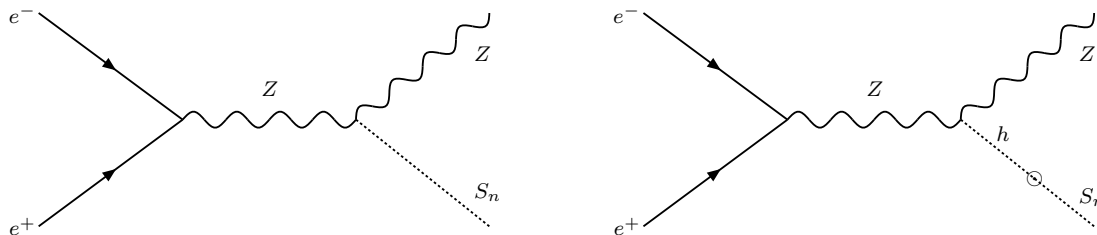


Figure 2: Feynman diagrams contributing to the process  $e^+e^- \rightarrow ZS_n$ .

The spin averaged squared matrix element for graviscalar (of mass  $m_n$ ) production at the  $e^+e^-$  collision via Higgs-strahlung (Feynman diagrams are shown in Fig. 2) is given by

$$\begin{aligned} \overline{\sum |\mathcal{M}|^2} &= \frac{g^2}{4M_P^2} \frac{(c_V^2 + c_A^2)}{\cos^2 \theta_W ((s - m_Z^2)^2 + m_Z^2 \Gamma_Z^2)} \left[ 2m_Z^2 s + 2(m_Z^2 - u)(m_Z^2 - t) \right] \\ &\times \left\{ \frac{g^2 m_{mix}^6}{((m_n^2 - m_h^2)^2 + m_h^2 \Gamma_h^2)} + \frac{\kappa^2 (1 - 6\xi)^2 \cos^2 \theta_W m_Z^2}{9} \right. \\ &\left. + \frac{2g m_{mix}^3 \kappa (1 - 6\xi) (m_n^2 - m_h^2) m_Z}{3((m_n^2 - m_h^2)^2 + m_h^2 \Gamma_h^2)} \right\}, \end{aligned} \quad (7)$$

where  $c_V$  and  $c_A$  are defined as in the coupling of an  $e^+e^-$  pair to a  $Z$ :  $g \gamma_\mu (c_V + c_A \gamma_5)$ .

The cross-section can be easily obtained from the above after a straightforward phase space integration. Finally we have to sum over the graviscalar tower to have the observable rate. It is, however, evident from Eq. (7), that the effect of mixing is most important for the graviscalar masses close to the Higgs mass.

The important point to note here is that a similar final state can arise in such a scenarios not only from the Standard Model contributions ( $ZZ/WW$ ) but also in the production of a  $Z$ -boson with towers of graviton (spin-2/spin-0). Therefore, a complete calculation on the prospects of the invisible Higgs signal has to take into account the continuum graviton production as well. This is a point that we wish to emphasize in the present study.

In our calculation, we have included, in addition to the SM processes  $e^+e^- \rightarrow ZZ/WW \rightarrow \mu^+\mu^- + \cancel{E}$ , gravitensor production together with a  $Z$ -boson, both leading to identical final states.

We use the following event selection criteria:

- $p_T^l > 10$  GeV,
- reject any  $M_{recoil}$  in the mass windows of  $m_Z \pm 5$  GeV and again  $(\sqrt{s} - m_Z) \pm 5$  GeV,

where  $M_{recoil}$  is defined as the mass of the system recoiling against the  $\mu^+\mu^-$  pair (which peak at the  $Z$ -boson mass). The second criterion is to reject the events originating from SM  $ZZ$  production and decay. This kinematic cut also eliminates the signal of an invisible Higgs, which is very close in mass to a  $Z$ -boson or of mass in the vicinity of  $(\sqrt{s} - m_Z)$ . It is well known that the Bjorken process is not very useful in searching for a Higgs boson close in mass to the  $Z$ . On the other hand, a part of the SM background comes from the production of an on-shell  $Z$  (subsequently decaying to a  $\mu^+\mu^-$  pair) along with two neutrinos. A peak in the recoil mass distribution around  $\sqrt{s} - m_Z$  corresponds to this particular configuration. Our choice of cut on the recoil mass helps to eliminate this component of background. It is needless to mention that, this cut also removes any signal of an invisibly decaying Higgs boson around this mass range. But we have investigated that beyond a mass of 250 GeV or so, our proposed method is not very effective. Even for a 500 GeV  $e^+e^-$  machine, the above cut will affect the Higgs signal beyond 400 GeV.

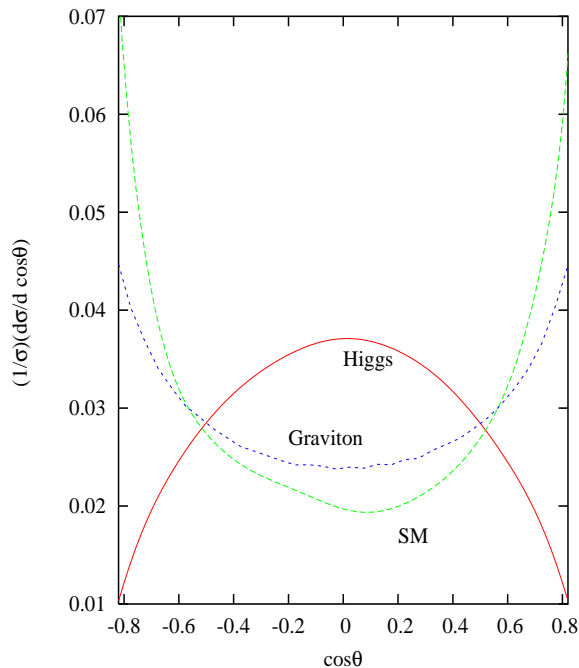


Figure 3: Angular distribution of invisible Higgs as reconstructed from the  $\mu^+\mu^-$  pair. The SM and gravitensor distributions are also shown.

We will now concentrate on the possible ways to filter out the Higgs effects from gravitensor and SM contributions. Though we are dealing with invisible decay products in the final state, the environment of an  $e^+e^-$  collider enables one to reconstruct the invisible system from the information of the visible decay products. Thus, by measuring the four-momenta of the final muons, we can reconstruct the mass of the system against which this  $\mu^+\mu^-$  are recoiling. In

the case of our interest, the recoil mass distribution peaks at the Higgs mass modulo the Higgs width and detector resolution. For the gravitensor production, the recoil mass distribution is a continuum, reflecting the monotonically increasing (quasi-) continuous density of graviton states with graviton mass. The SM contribution, as has been already mentioned, has two main channels, namely,  $e^+e^- \rightarrow ZZ$  and  $e^+e^- \rightarrow W^+W^-$ . If now nature has chosen to have large extra dimensions with non-negligible Higgs-graviscalar mixing, then the recoil mass distribution in our process of interest will show a continuum due to gravitensor and SM with characteristic peaks of Higgs boson superposed on it. The position of this peak will be determined by the Higgs mass. Now emerges a crucial issue: the height of this peak. Height of this peak is determined, apart from other parameters, by the Higgs-graviscalar mixing  $\xi$ , the same quantity which also determines the Higgs width, making the width large for  $\xi = O(1)$ . As has already been pointed out, this causes the invisible decay recoil mass distribution to lose its sharp character even for a Higgs mass on the order of 120 GeV. A larger width will essentially spread out the Higgs contribution to a number of recoil mass bins (centered around the Higgs mass) and thereby weaken the signal.

One way out of the problem is to use angular distributions which are drastically different for Higgs production as compared to SM and gravitensor production. If we concentrate on the distribution of the scattering angle of the  $\mu^+\mu^-$  system, for Higgs production this is peaked around the central part of the detector in contrast to the graviton and the SM cases, where these are peaked around the forward and backward directions with respect to the initial electron beam. This can be accounted for by the t- and u- channel electron propagators in SM and gravitensor production, particularly, when a photon (in case of SM) or a very light (nearly massless) graviton is attached to the electron line. In other words, mass of the final state particle (other than the Z-boson) and also the demand of a minimum  $p_T$  of the final state particles, acts as a regulator to this singularity of cross-section in extreme forward/backward direction.

In Fig. 3, we present the normalised angular distributions for above three cases. The figure indicates that an angular cut can be used to disentangle the two new physics effects from each other, and at the same time to reduce the SM backgrounds. The Higgs signal is filtered quite effectively if we apply the following cut on the relevant angle :  $|\cos\theta| < 0.8$ . This selection criteria, killing almost 50 % of the SM and graviton production, leaves us with a prominent invisible Higgs signal, at least for a Higgs mass on the lower side.

However, even this angular cut is not of much help for higher Higgs masses. This is due to twofold reasons. First, the production cross-section itself decreases with rise in the Higgs mass. The second and more important reason, however, is the sharp increase of Higgs width with Higgs mass. For a 200 GeV Higgs boson, Higgs width is quite large due to opening up of  $WW, ZZ$  decay channels. At the same time the invisible branching ratio can be substantial and even dominant, as is indicated by Fig. 1. Consequently, the recoil mass is spread over a larger number of bins, thus flattening out the peak. This effect is more damaging for our signal the higher the Higgs mass is.

The above conclusions are borne out in Fig. 4 where we have plotted the recoil mass distribution (as discussed above) for the  $\mu^+\mu^- + \text{missing energy}$  events including the SM, gravitensor and invisibly decaying Higgs production. The results are presented for three different values of the number of extra dimensions. In the two sets of plots, corresponding to Higgs masses 120 GeV (left) and 200 GeV (right), respectively, the different degrees of visibility of the peak is quite obvious, because of reasons discussed above. For the purpose of illustration, we have chosen  $m_D = 1.5$  TeV,  $\xi = 1$  and  $\sqrt{s} = 1$  TeV. To take into account a realistic detector resolution

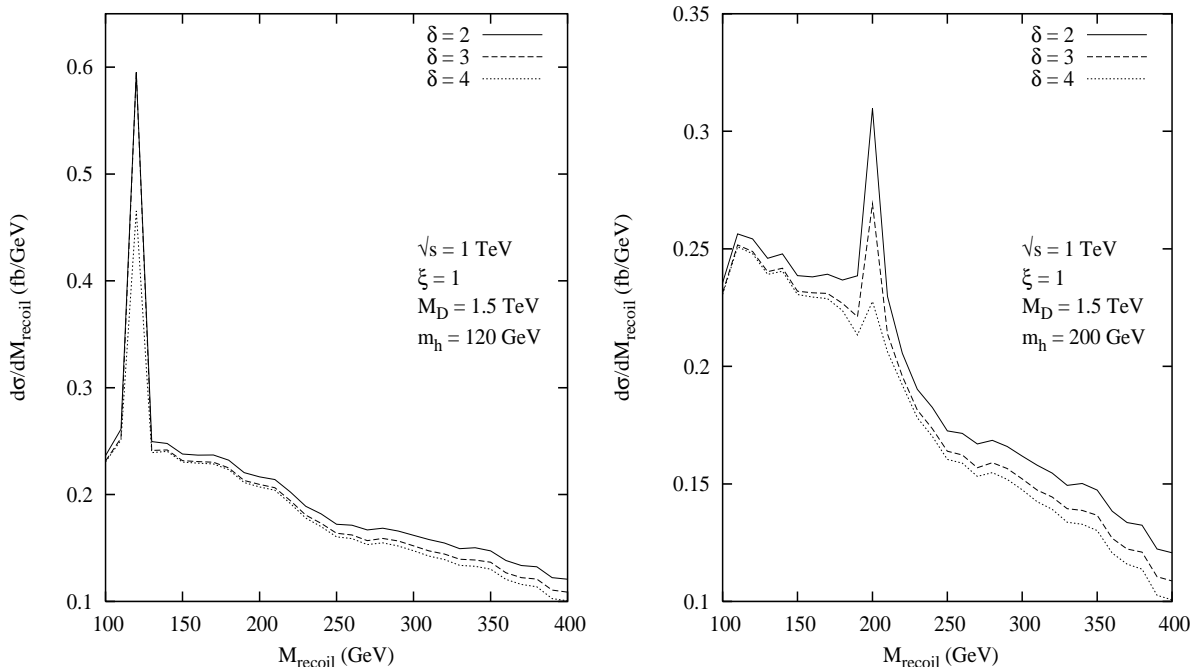


Figure 4: Recoil mass distribution for invisible Higgs for different values of  $\delta$ , superposed over the SM and gravitensor contributions, for  $m_D = 1.5$  TeV and  $\xi = 1$ .

we have assumed a Gaussian spreading of muon energy:  $\Delta E/E = 0.15/\sqrt{E} + 0.01$  [14]. The visibility of the peak for the lower Higgs mass is largely due to the angular cut. For a heavier Higgs, however, reconstruction of the peak appears to be difficult.

The visibility of the proposed signal depends on the relative rates of the invisible Higgs decay channel and the SM and gravitensor continuum channels. The standard procedure in such a situation is to compare the number of Higgs signal events to the square root of the number of events coming from the 'background' in the particular mass bin, in which we see the peak. There are two caveats to this criteria. The number of background (and signal) events should be sufficiently large so that square root of this number represents  $1\sigma$  fluctuation of the background (in Gaussian statistics). Secondly, we also must know the absolute normalization of the background very well. While the first criterion can be satisfied with high luminosity, the second one, in our case, poses a problem. There is a part of the number of events coming from gravitensor production. This depends on unknown parameters like  $\delta$  and  $m_D$ , and thus is correlated with the number of signal (invisible Higgs) events via these parameters.

In Table 2, we present the cross-sections of  $\mu^+\mu^- +$  missing momentum final state from three different sources separately. Instead of the total rates, the cross-sections in a particular mass bin (of width 10 GeV) are more appropriate for our discussion and have been presented in the tables. We choose two different Higgs masses: 120 GeV and 200 GeV. Looking at the numbers in the table one can readily appreciate the smallness of gravitensor contributions to the relevant bins, in contrast to the SM contributions.

Let us make some further comments about the numbers in the table. The monotonic decrease of cross-sections (in a particular mass bin for a fixed value of  $m_D$  and  $s_{ee}$ ) with increasing values

of  $\delta$  for invisible Higgs<sup>2</sup> and gravitensor is due to steady decrease of available number density of graviscalar/tensor states as pointed out earlier. Invisible Higgs cross-section also decreases with  $e^+e^-$  center-of-mass energy (compare any two corresponding entries for two tables). This can be accounted by the s-channel propagators in the two contributing diagrams (Fig. 2). On the other hand, decrease of graviton (spin-2) contribution to mass bins is modest with center-of-mass energy. There are four graphs contributing to this spin-2 production (along with a  $Z$ -boson). The s-channel contribution goes down as usual when we go to a higher center of mass energy. This fall is somehow compensated by a four-point contact graph and we are left with a modest decrement in the cross-section with  $e^+e^-$  center-of-mass energy. It is also to be noted that while the invisible Higgs contributions to the final state fall for higher center-of-mass energy, the gravitensor contribution remains practically unchanged. This is because the latter involves an integration over the entire tower that is kinematically available, and a higher value of  $\sqrt{s}$  allows one to integrate over a bigger tower. For the invisible Higgs signal, however, this does not make any difference, since the dominant contribution there comes from that portion of the graviscalar tower which is close to the Higgs mass. Therefore, the signature of scalar-graviscalar mixing stands out more prominently for a linear collider operating at 500 GeV than one at 1 TeV.

## 4 Summary and conclusions

We have investigated the detection prospects of a Higgs boson that has mixing with a quasi-continuous tower of graviscalars in a scenario with large compact extra dimensions. This causes the Higgs to develop an invisible decay width. In the context of a linear  $e^+e^-$  collider, however, such invisibility brings in additional problems in reconstructing the Higgs boson as a recoil mass peak against an identified Higgs boson. This is because of (a) the simultaneous presence of graviton continuum production in association with a  $Z$ -boson, and (b) the broadening of the Higgs peak due to enhancement of the total effective decay width. We find that while a judicious angular cut partially alleviated the difficulty, the broadening of the peak remains a problem, particularly for  $m_H > 2m_W$ . Therefore, the search for a Higgs boson in a scenario of this kind, and more importantly, the detailed investigation of its properties, has wider ramification than an invisibly decaying Higgs envisioned in most other models.

When this work was nearing its completion, a corresponding study in the context of LHC [15] appeared in the literature, where an attempt has been made to point out the detectability of a light invisible Higgs in the ADD-model hadron colliders in the gauge boson fusion channel. However, a complete answer is not yet available on whether continuum graviton production can be a problem here, too, since such production can take place even in gluon fusion. Therefore, our view is that a full estimate of direct gravitensor and graviscalar production rates giving rise to the same final states is required before a conclusion can be reached on the signature Higgs-graviscalar mixing. We are also aware of [16], where invisible Higgs in linear colliders has been considered for  $Z$  decaying to a quark pair. Again, the difficulties arising from direct graviton

---

<sup>2</sup>The only exception is when going from  $\delta = 2$  to  $\delta = 3$  for  $m_h = 120$  GeV,  $\sqrt{s} = 1$  TeV, and  $m_D = 1.5$  TeV. The slightly decreasing cross section for this particular parameter set is due to the interplay of density of graviscalar states and a large portion of invisible Higgs partial width in the total width in Eq. (7).

Cross-sections (fb) in bin of width 10 GeV; $\sqrt{s_{ee}} = 0.5$ TeV							
recoil mass bin		$m_D = 1.5$ TeV			$m_D = 3$ TeV		
		$\delta = 2$	$\delta = 3$	$\delta = 4$	$\delta = 2$	$\delta = 3$	$\delta = 4$
$120 \pm 5$ GeV	IH:	1.488	1.485	1.155	1.311	0.592	0.075
	GT:	$6.6 \times 10^{-3}$	0.001	0.0001	$4.4 \times 10^{-4}$	$3.3 \times 10^{-5}$	$2 \times 10^{-6}$
	SM:	1.95	1.95	1.95	1.95	1.95	1.95
$200 \pm 5$ GeV	IH:	0.321	0.205	0.070	0.041	0.009	0.001
	GT:	0.013	0.0036	$7.4 \times 10^{-4}$	$8.3 \times 10^{-4}$	$1.1 \times 10^{-4}$	$1.1 \times 10^{-5}$
	SM:	0.873	0.873	0.873	0.873	0.873	0.873
$300 \pm 5$ GeV	IH:	0.067	0.059	0.035	0.011	0.0037	0.00075
	GT:	0.0311	0.0125	0.0039	$1.9 \times 10^{-3}$	$3.9 \times 10^{-4}$	$6.1 \times 10^{-5}$
	SM:	0.297	0.297	0.297	0.297	0.297	0.297

Cross-sections (fb) in bin of width 10 GeV; $\sqrt{s_{ee}} = 1$ TeV							
recoil mass bin		$m_D = 1.5$ TeV			$m_D = 3$ TeV		
		$\delta = 2$	$\delta = 3$	$\delta = 4$	$\delta = 2$	$\delta = 3$	$\delta = 4$
$120 \pm 5$ GeV	IH:	0.341	0.346	0.217	0.219	0.093	0.011
	GT:	0.0058	$9.2 \times 10^{-4}$	$1.1 \times 10^{-4}$	$3.6 \times 10^{-4}$	$2.9 \times 10^{-5}$	$1.8 \times 10^{-6}$
	SM:	0.247	0.247	0.247	0.247	0.247	0.247
$200 \pm 5$ GeV	IH:	0.093	0.059	0.020	0.012	0.0027	0.0003
	GT:	$9.8 \times 10^{-3}$	0.0028	0.0005	$6.5 \times 10^{-4}$	$8.7 \times 10^{-5}$	$8.2 \times 10^{-6}$
	SM:	0.206	0.206	0.206	0.206	0.206	0.206
$300 \pm 5$ GeV	IH:	0.035	0.03	0.018	0.006	0.002	0.00038
	GT:	0.016	0.0065	0.0021	$1.1 \times 10^{-3}$	$2.0 \times 10^{-4}$	$3.4 \times 10^{-5}$
	SM:	0.145	0.145	0.145	0.145	0.145	0.145

Table 2: Cross-sections in the relevant bins of recoil mass (of the system recoiling against  $\mu^+\mu^-$  pair) for invisible Higgs (IH), gravitensor (GT) and the Standard Model (SM) for  $e^+e^-$  center of mass energy of 0.5 and 1 TeV. Entries in the left-most columns of each table indicate the central values and widths of the mass bins, we are interested. For IH, the central value of the recoil mass bin indicates the Higgs mass.

production need to be addressed before reaching a verdict in such a study.

## Acknowledgments

AD, KH and JL thank the Academy of Finland (project numbers 48787, 104368, and 54023) for financial support. BM wishes to acknowledge the hospitality of Katri Huitu and the Helsinki Institute of Physics at the time when this work was initiated.

## References

- [1] R.E. Shrock, M. Suzuki, Phys. Lett. **B110** (1982) 250; A.S. Joshipura, J.W.F. Valle, Nucl. Phys. **B397** (1993) 105.
- [2] J.F. Gunion, Phys. Rev. Lett. **72** (1994) 199; S.G. Frederiksen, N. Johnson, G.L. Kane, J. Reid, Phys. Rev. **D50** (1994) 4244.
- [3] O.J.P. Eboli, D. Zeppenfeld, Phys. Lett. **B495** (2000) 147.
- [4] G. Belanger, F. Boudjema, F. Donato, R.M. Godbole, S. Rosier-Lees, Nucl. Phys. **B581** (2000) 3; G. Belanger, F. Boudjema, A. Cottrant, R.M. Godbole, A. Semenov, Phys. Lett. **B519** (2001) 93; K. Griest, H.E. Haber, Phys. Rev. **D37** (1988) 719.
- [5] A. Joshipura, S.D. Rindani, Phys. Rev. Lett. **69** (1992) 3269; A. Datta, A. Raychaudhuri, Phys. Rev. **D57** (1998) 2940.
- [6] D. Choudhury, D.P. Roy, Phys. Lett. **B322** (1994) 368; R.M. Godbole, M. Guchait, K. Mazumdar, S. Moretti, D.P. Roy, Phys. Lett. **B571** (2003) 184.
- [7] G.F. Giudice, R. Rattazzi and J.D. Wells, Nucl. Phys. **B595** (2001) 250.
- [8] N. Arkani-Hamed, S. Dimopoulos, G. Dvali, J. March-Russell, Phys. Rev. **D65** (2002) 024032; S. Martin, J.D. Wells, Phys. Rev. **D60** (1999) 035006; N.G. Deshpande, D.K. Ghosh, Phys. Lett. **B567** (2003) 235.
- [9] N. Arkani-Hamed, S. Dimopoulos and G. Dvali, Phys. Lett. **B429** (1998) 263; I. Antoniadis, N. Arkani-Hamed, S. Dimopoulos and G. R. Dvali, Phys. Lett. **B436**, (1998) 257
- [10] L. Randall and R. Sundrum, Phys. Rev. Lett. **83**(1999) 3370; *ibid* **83** (1999) 4690.
- [11] T. Han, G.D. Kribs, B. McElrath, Phys. Rev. **D64** (2001) 076003; M. Chaichian, A. Datta, K. Huitu, Z.-H. Yu, Phys. Lett. **B524** (2002) 161; J.L. Hewett, T.G. Rizzo, JHEP **0308** (2003) 028; D. Dominici, B. Grzadkowski, J.F. Gunion, M. Toharia, Nucl. Phys. **B671** (2003) 243; K. Cheung, C.S. Kim, J.-H. Song, Phys. Rev. **D67** (2003) 075017; hep-ph/0311295; A. Datta, K. Huitu, Phys. Lett. **B578** (2004) 376.
- [12] The LEP working group for Higgs boson studies, LHWG Note 2001-06, hep-ex/0107032.
- [13] M. Spira, P. Zerwas, hep-ph/9803257.

- [14] H. Murayama, M. Peskin, *Ann. Rev. Nucl. Part. Sci.* **46** (1996) 533.
- [15] M. Battaglia, D. Dominici, J.F. Gunion, J.D. Wells, hep-ph/0402062.
- [16] M. Schumacher, LC-PHSM-2003-096.